

STAR Detector Overview

K.H. Ackermann^p, N. Adams^x, C. Adler^k, Z. Ahammed^w,
S. Ahmad^x, C. Allgower^ℓ, J. Amonettⁿ, J. Amsbaugh^{ad},
B.D. Andersonⁿ, M. Anderson^e, E. Anderssen^o, H. Arnesen^b,
L. Arnoldⁿ, G.S. Averichevⁱ, A. Baldwinⁿ, J. Balewski^ℓ,
O. Barannikova^{i,w}, L.S. Barnbyⁿ, J. Baudot^m, M. Beddo^a,
S. Bekele^t, V.V. Belagaⁱ, R. Bellwied^{ae}, S. Bennett^{ae},
J. Bercovitz^o, J. Berger^k, W. Betts^b, H. Bichsel^{ad}, F. Bieser^o,
L.C. Bland^b, M. Bloomer^o, C.O. Blyth^c, J. Boehm^o, B.E. Bonner^x,
D. Bonnet^m, R. Bossingham^o, M. Botlo^b, A. Boucham^z,
N. Bouillo^z, S. Bouvier^z, K. Bradley^o, F.P. Brady^e, A. Brandin^r,
R. L. Brown^b, G. Brugalette^{ad}, M. Burkes^o, R.V. Cadman^a,
H. Caines^{ag}, M. Calderón de la Barca Sánchez^b, A. Cardenas^w,
L. Carr^{ad}, J. Carroll^o, J. Castillo^z, M. Castro^{ae}, D. Cebra^e,
S. Chattopadhyay^{ae}, M.L. Chen^b, W. Chen^b, Y. Chen^f,
S.P. Chernenkoⁱ, M. Cherney^h, A. Chikanian^{ag}, B. Choi^{ab},
J. Chrin^h, W. Christie^b, J.P. Coffin^m, L. Conin^z, C. Consiglio^b,
T.M. Cormier^{ae}, J.G. Cramer^{ad}, H.J. Crawford^d, I. Danilovⁱ,
D. Dayton^b, M. DeMello^x, W.S. Deng^b, A.A. Derevschikov^v,
M. Dialinas^z, H. Diaz^b, P.A. DeYoung^g, L. Didenko^b,
D. Dimassimo^b, J. Dioguardi^b, C. Drancourt^z, T. Dietel^k,
J.E. Draper^e, V.B. Duninⁱ, J.C. Dunlop^{ag}, V. Eckardt^p,
W.R. Edwards^o, L.G. Efimovⁱ, T. Eggert^p, V. Emelianov^r,
J. Engelage^d, G. Eppley^x, B. Erazmus^z, A. Etkin^b, P. Fachini^b,
V. Faine^b, C. Feliciano^b, D. Ferenc^e, M.I. Ferguson^f, H. Fessler^p,
K. Filimonov^o, E. Finch^{ag}, Y. Fisyak^b, D. Flierl^k, I. Flores^d,
K.J. Foley^b, D. Fritz^o, J. Fu^o, C.A. Gagliardi^{aa}, N. Gagunashviliⁱ,
J. Gans^{ag}, L. Gaudichet^z, M. Gazdzicki^ℓ, M. Germain^m,
F. Geurts^x, V. Ghazikhanian^f, C. Gojak^m, J. Grabski^{ac},
O. Grachov^{ae}, M. Grau^b, D. Greiner^o, L. Greiner^d, V. Grigoriev^r,
D. Grosnick^a, J. Gross^h, M. Guedon^m, G. Guilloux^z, E. Gushin^r,
J. Hall^{ae}, T.J. Hallman^b, D. Hardtke^o, G. Harper^{ad}, J.W. Harris^{ag},
M. Heffner^e, S. Heppelmann^u, T. Herston^w, D. Hill^a,

B. Hippolyte^m, A. Hirsch^w, E. Hjort^o, G.W. Hoffmann^{ab},
 M. Horsley^{ag}, M. Howe^{ad}, H.Z. Huang^f, T.J. Humanic^t,
 H. Hümmler^p, W. Hunt^l, J. Hunter^o, G. Igo^f, A. Ishihara^{ab},
 Yu.I. Ivanshin^j, P. Jacobs^o, W.W. Jacobs^l, S. Jacobson^o,
 M. Janik^{ac}, R. Jared^o, P. Jensen^{ab}, I. Johnson^o, P.G. Jones^c,
 E.G. Judd^d, M. Kaneta^o, M. Kaplan^g, D. Keaneⁿ, A. Khodinov^r,
 J. Kiryluk^f, A. Kisiel^{ac}, J. Klay^o, S.R. Klein^o, A. Klyachko^l,
 G. Koehler^o, A.S. Konstantinov^v, I. Kotov^t, M. Kopytineⁿ,
 L. Kotchenda^r, A.D. Kovalenkoⁱ, M. Kramer^s, P. Kravtsov^r,
 K. Krueger^a, T. Krupien^b, P. Kuczewski^b, C. Kuhn^m,
 A.I. Kulikovⁱ, G.J. Kunde^{ag}, C.L. Kunz^g, R. Kh. Kutuev^j,
 A.A. Kuznetsovⁱ, L. Lakehal-Ayat^z, M.A.C. Lamont^c,
 J.M. Landgraf^b, S. Lange^k, C.P. Lansdell^{ab}, B. Lasiuk^{ag}, F. Laue^b,
 A. Lebedev^b, T. LeCompte^a, R. Lednickýⁱ, W.J. Leonhardt^b,
 V.M. Leontiev^v, M.J. LeVine^b, Q. Li^{ae}, C.-J. Liaw^b, J. Lin^h,
 S.J. Lindenbaum^s, V. Lindenstruth^o, P.J. Lindstrom^d, M.A. Lisa^t,
 F. Liu^{af}, L. Liu^{af}, Z. Liu^{af}, Q.J. Liu^{ad}, T. Ljubicic^b, W.J. Llope^x,
 G. LoCurto^p, H. Long^f, R.S. Longacre^b, M. Lopez-Noriega^t,
 W.A. Love^b, D. Lynn^b, R. Maier^p, R. Majka^{ag}, S. Margetisⁿ,
 C. Markert^{ag}, L. Martin^z, J. Marx^o, H.S. Matis^o,
 Yu.A. Matulenko^v, C. McParland^o, T.S. McShane^h, J. Meier^h,
 F. Meissner^o, Yu. Melnick^v, A. Meschanin^v, M. Messer^b,
 P. Middlekamp^b, B. Miller^b, M.L. Miller^{ag}, Z. Milosevich^g,
 N.G. Minaev^v, B. Minor^o, J. Mitchell^x, E. Mogavero^b,
 V.A. Moiseenko^j, D. Moltz^o, C.F. Moore^{ab}, V. Morozov^o,
 M.M. de Moura^{ae}, M.G. Munhoz^y, G.S. Mutchler^x, J.M. Nelson^c,
 P. Nevski^b, M. Nguyen^b, T. Nguyen^b, V.A. Nikitin^j, L.V. Nogach^v,
 T. Noggle^o, B. Normanⁿ, S.B. Nurushev^v, T. Nussbaum^x,
 J. Nystrand^o, G. Odyniec^o, A. Ogawa^u, C.A. Ogilvie^l,
 V. Okorokov^r, K. Olchanski^b, M. Oldenburg^p, D. Olson^o, G. Ott^{ab},
 D. Padrazo^b, G. Paic^t, S.U. Pandey^b, Y. Panebratsevⁱ,
 S.Y. Panitkin^b, A.I. Pavlinov^{ae}, T. Pawlak^{ac}, V. Perevoztchikov^b,
 W. Peryt^{ac}, V.A. Petrov^j, W. Pinganaud^z, S. Pirogov^f, E. Platner^x,
 J. Pluta^{ac}, I. Polk^b, N. Porile^w, J. Porter^b, A.M. Poskanzer^o,
 E. Potrebenikovaⁱ, D. Prindle^{ad}, C. Pruneau^{ae}, J. Puskar-Pasewicz^l,

G. Rai ^o, J. Rasson ^o, O. Ravel ^z, R.L. Ray ^{ab}, S.V. Razin ^{i,ℓ},
 D. Reichhold ^h, J.G. Reid ^{ad}, R.E. Renfordt ^k, F. Retiere ^o,
 A. Ridiger ^r, J. Riso ^{ae}, H.G. Ritter ^o, J.B. Roberts ^x, D. Roehrich ^k,
 O.V. Rogachevski ⁱ, J.L. Romero ^e, C. Roy ^z, D. Russ ^g, V. Rykov ^{ae},
 I. Sakrejda ^o, R. Sanchez ^f, Z. Sandler ^f, S. Salur ^{ag}, J. Sandweiss ^{ag},
 A.C. Saulys ^b, I. Savin ^j, J. Schambach ^{ab}, R.P. Scharenberg ^w,
 J. Scheblien ^b, R. Scheetz ^b, R. Schlueter ^o, N. Schmitz ^p,
 L.S. Schroeder ^o, M. Schulz ^b, A. Schüttauf ^p, K. Schweda ^o,
 J. Sedlmeir ^b, J. Seger ^h, D. Seliverstov ^r, P. Seyboth ^p,
 R. Seymour ^{ad}, E. Shahaliev ⁱ, K.E. Shestermanov ^v,
 S.S. Shimanskii ⁱ, D. Shuman ^o, V.S. Shvetcov ^j, G. Skoro ⁱ,
 N. Smirnov ^{ag}, L.P. Smykov ⁱ, R. Snellings ^o, K. Solberg ^ℓ,
 P. Sorensen ^f, J. Sowinski ^ℓ, H.M. Spinka ^a, B. Srivastava ^w,
 E.J. Stephenson ^ℓ, R. Stock ^k, A. Stolpovsky ^{ae}, N. Stone ^b,
 M. Strikhanov ^r, B. Stringfellow ^w, H. Stroebele ^k, C. Struck ^k,
 A.A.P. Suaide ^{ae}, E. Sugarbaker ^t, C. Suire ^m, M. Šumbera ^t,
 T.J.M. Symons ^o, A. Szanto de Toledo ^y, P. Szarwas ^{ac}, A. Tai ^f,
 J. Takahashi ^y, A.H. Tang ⁿ, A. Tarchini ^m, J. Tarzian ^o,
 J.H. Thomas ^o, M. Thompson ^c, V. Tikhomirov ^r, M. Tokarev ⁱ,
 M.B. Tonjes ^q, S. Tonse ^o, T.A. Trainor ^{ad}, S. Trentalange ^f,
 R.E. Tribble ^{aa}, V. Trofimov ^r, O. Tsai ^f, K. Turner ^b, T. Ullrich ^b,
 D.G. Underwood ^a, I. Vakula ^f, G. Van Buren ^b,
 A.M. VanderMolen ^q, A. Vanyashin ^o, I.M. Vasilevski ^j,
 A.N. Vasiliev ^v, S.E. Vigdor ^ℓ, G. Visser ^d, S.A. Voloshin ^{ae}, C. Vu ^o,
 F. Wang ^w, H. Ward ^{ab}, J.W. Watson ⁿ, D. Weerasundara ^{ad},
 R. Weidenbach ^o, R. Wells ^t, T. Wenaus ^b, G.D. Westfall ^q,
 J.P. Whitfield ^g, C. Whitten Jr. ^f, H. Wieman ^o, R. Willson ^t,
 K. Wilson ^{ae}, J. Wirth ^o, J. Wisdom ^f, S.W. Wissink ^ℓ, R. Witt ^{ag},
 J. Wolf ^o, J. Wood ^f, N. Xu ^o, Z. Xu ^b, A.E. Yakutin ^v,
 E. Yamamoto ^o, J. Yang ^f, P. Yepes ^x, A. Yokosawa ^a, V.I. Yurevich ⁱ,
 Y.V. Zanevski ⁱ, I. Zborovský ⁱ, H. Zhang ^{ag}, W.M. Zhang ⁿ,
 D. Zimmerman ^o, R. Zoulkarneev ^j, A.N. Zubarev ⁱ

(STAR Collaboration)

^aArgonne National Laboratory, Argonne, Illinois 60439

^bBrookhaven National Laboratory, Upton, New York 11973

- ^c*University of Birmingham, Birmingham, United Kingdom*
- ^d*University of California, Berkeley, California 94720*
- ^e*University of California, Davis, California 95616*
- ^f*University of California, Los Angeles, California 90095*
- ^g*Carnegie Mellon University, Pittsburgh, Pennsylvania 15213*
- ^h*Creighton University, Omaha, Nebraska 68178*
- ⁱ*Laboratory for High Energy (JINR), Dubna, Russia*
- ^j*Particle Physics Laboratory (JINR), Dubna, Russia*
- ^k*University of Frankfurt, Frankfurt, Germany*
- ^l*Indiana University, Bloomington, Indiana 47408*
- ^m*Institut de Recherches Subatomiques, Strasbourg, France*
- ⁿ*Kent State University, Kent, Ohio 44242*
- ^o*Lawrence Berkeley National Laboratory, Berkeley, California 94720*
- ^p*Max-Planck-Institut fuer Physik, Munich, Germany*
- ^q*Michigan State University, East Lansing, Michigan 48824*
- ^r*Moscow Engineering Physics Institute, Moscow Russia*
- ^s*City College of New York, New York City, New York 10031*
- ^t*Ohio State University, Columbus, Ohio 43210*
- ^u*Pennsylvania State University, University Park, Pennsylvania 16802*
- ^v*Institute of High Energy Physics, Protvino, Russia*
- ^w*Purdue University, West Lafayette, Indiana 47907*
- ^x*Rice University, Houston, Texas 77251*
- ^y*Universidade de Sao Paulo, Sao Paulo, Brazil*
- ^z*SUBATECH, Nantes, France*
- ^{aa}*Texas A & M, College Station, Texas 77843*
- ^{ab}*University of Texas, Austin, Texas 78712*
- ^{ac}*Warsaw University of Technology, Warsaw, Poland*
- ^{ad}*University of Washington, Seattle, Washington 98195*
- ^{ae}*Wayne State University, Detroit, Michigan 48201*
- ^{af}*Institute of Particle Physics, Wuhan, Hubei 430079 China*
- ^{ag}*Yale University, New Haven, Connecticut 06520*

Abstract

An introduction to the STAR detector and a brief overview of the physics goals of the experiment are presented.

1 Introduction

The Solenoidal Tracker at RHIC (STAR) is one of two large detector systems constructed at the Relativistic Heavy Ion Collider (RHIC) at Brookhaven National Laboratory.

There are eighteen articles in this volume that describe the STAR detector. They are:

- STAR Detector Overview (This article)
- The STAR Detector Magnet System
- The STAR Silicon Vertex Tracker
- The STAR Silicon Strip Detector
- The STAR Time Projection Chamber
- The Readout System for the STAR Time Projection Chamber
- The Laser System for the STAR Time Projection Chamber
- The STAR TPC Gas System
- The Forward Time Projection Chamber in STAR
- Identification of High p_t Particles with the STAR-RICH Detector
- The STAR Barrel Electromagnetic Calorimeter
- The STAR Endcap Electromagnetic Calorimeter
- The STAR Photon Multiplicity Detector
- An Overview of the STAR DAQ System
- The STAR Trigger
- The STAR Level-3 Trigger System
- Hardware Controls for the STAR Experiment at RHIC
- Integration and Conventional Systems at STAR

STAR was constructed to investigate the behavior of strongly interacting matter at high energy density and to search for signatures of quark-gluon plasma (QGP) formation. Key features of the nuclear environment at RHIC are a large number of produced particles (up to approximately one thousand per unit pseudo-rapidity) and high momentum particles from hard parton-parton scattering. STAR will measure many observables simultaneously to study signatures of a possible QGP phase transition and to understand the space-time evolution of the collision process in ultra-relativistic heavy ion collisions. The goal is to obtain a fundamental understanding of the microscopic structure of these hadronic interactions at high energy densities.

¹ Presently at Iowa State University, Ames, Iowa 50011

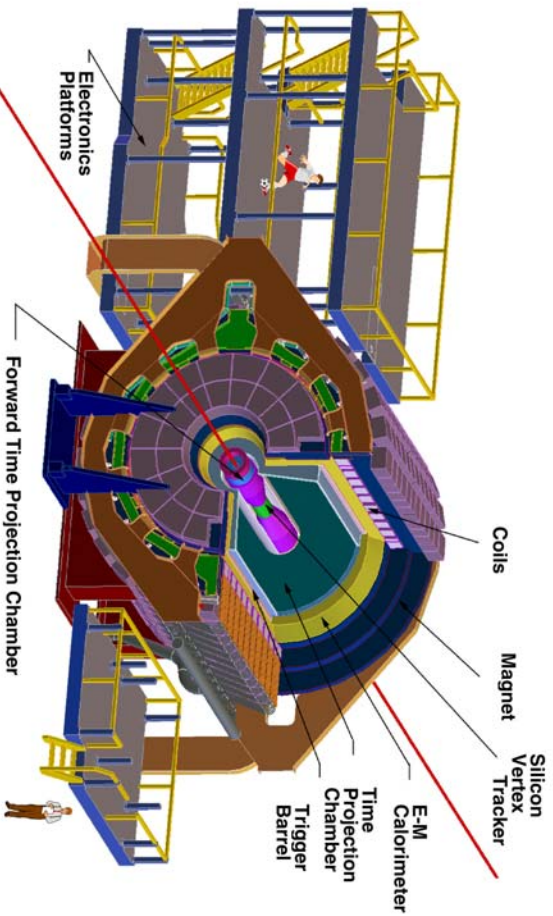


Fig. 1. Perspective view of the STAR detector, with a cutaway for viewing inner detector systems.

2 Detector Overview

In order to accomplish this, STAR was designed primarily for measurements of hadron production over a large solid angle, featuring detector systems for high precision tracking, momentum analysis, and particle identification at the center of mass (c.m.) rapidity. The large acceptance of STAR makes it particularly well suited for event-by-event characterizations of heavy ion collisions and for the detection of hadron jets.

The layout of the STAR experiment [1] is shown in Figure 1. A cutaway side view of the STAR detector as configured for the RHIC 2001 run is displayed in Figure 2. A room temperature solenoidal magnet[2] with a maximum magnetic field of 0.5 T provides a uniform magnetic field for charged particle momentum analysis. Charged particle tracking close to the interaction region is accomplished by a Silicon Vertex Tracker[3] (SVT) consisting of 216 silicon drift detectors (equivalent to a total of 13 million pixels) arranged in three cylindrical layers at distances of approximately 7, 11 and 15 cm from the beam axis. In the near future, a 4th layer of Silicon Drift Detectors[4] (SDD) will be added to the inner tracker. The silicon detectors cover a pseudo-rapidity range $|\eta| \leq 1$ with complete azimuthal symmetry ($\Delta\phi = 2\pi$). Silicon tracking close to the interaction allows precision localization of the primary interaction vertex and identification of secondary vertices from weak decays of, for example, Λ , Ξ , and Ω s. A large volume Time Projection Chamber[5] (TPC) for charged particle tracking and particle identification is located at a radial distance from 50 to 200 cm from the beam axis. The TPC is 4 meters long and it covers a pseudo-rapidity range $|\eta| \leq 1.8$ for tracking with complete azimuthal symmetry ($\Delta\phi = 2\pi$) providing the equivalent of 70 million voxels via 136,608

channels of front end electronics[6] (FEE). Both the SVT and TPC contribute to particle identification using ionization energy loss, with an anticipated combined energy loss resolution (dE/dx) of 7 % (σ). The momentum resolution of the SVT and TPC reach a value of $\delta p/p = 0.02$ for a majority of the tracks in the TPC. The $\delta p/p$ resolution improves as the number of hit points along the track increases and as the particle's momentum decreases, as expected.

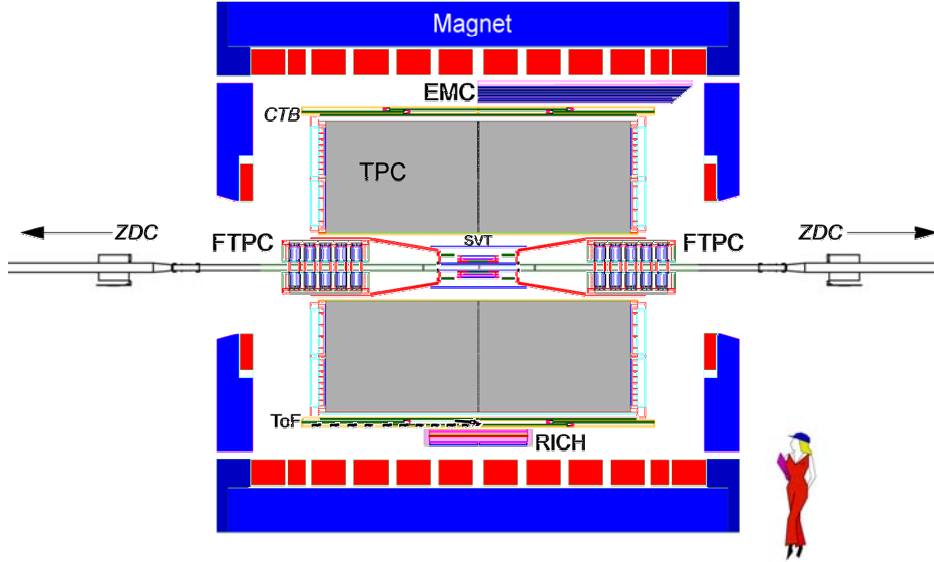


Fig. 2. Cutaway side view of the STAR detector as configured in 2001.

To extend the tracking to the forward region, a radial-drift TPC (FTPC)[7] is installed covering $2.5 < |\eta| < 4$, also with complete azimuthal coverage and symmetry. To extend the particle identification in STAR to larger momenta over a small solid angle for identified single-particle spectra at mid-rapidity, a ring imaging Cherenkov detector [8] covers $|\eta| < 0.3$ and $\Delta\phi = 0.11\pi$, and a time-of-flight (TOF) patch covers $-1 < \eta < 0$ and $\Delta\phi = 0.04\pi$ (as shown in Figure 2). About 10 percent of the full-barrel electromagnetic calorimeter[9] (EMC) shown in Figure 1 was installed for 2001 (see Figure 2). The remaining EMC and an endcap electromagnetic calorimeter[10] (EEMC) will be installed over the next three years to obtain an eventual coverage of $-1 < \eta < 2$ and $\Delta\phi = 2\pi$. This system will allow measurement of the transverse energy of events, and trigger on and measure high transverse momentum photons, electrons, and electromagnetically decaying hadrons. The EMC's include shower-maximum detectors to distinguish high momentum single photons from photon pairs resulting from π and η meson decays. The EMC's will also provide prompt charged particle signals essential to discriminate against pileup tracks in the TPC, arising from other beam crossings falling within the $40 \mu\text{sec}$ drift time of the TPC, which are anticipated to be prevalent at RHIC pp collisions luminosities ($\approx 10^{32} \text{cm}^{-2} \text{s}^{-1}$).

3 DAQ and Triggering

The STAR data acquisition system[11] (DAQ) is fast and flexible. It receives data from multiple detectors and these detectors have a wide range of readout rates. The event size is of order 200 MB and the events are processed at input rates up to 100 Hz.

The STAR trigger system[12] is a 10 MHz pipelined system which is based on input from fast detectors to control the event selection for the much slower tracking detectors. The trigger system is functionally divided into different layers with level 0 being the fastest while level 1 and level 2 are slower but they apply more sophisticated constraints on the event selection.

STAR has a third level trigger[13] which performs complete online reconstruction of the events in a dedicated CPU farm. The level 3 trigger can process central Au-Au collisions at a rate of 50 Hz including simple analysis of physics observables such as particle momentum and rate of energy loss. The level 3 trigger system includes an online display so that individual events can be visually inspected in real time. See Fig. 3 for an end view of an event in the TPC.

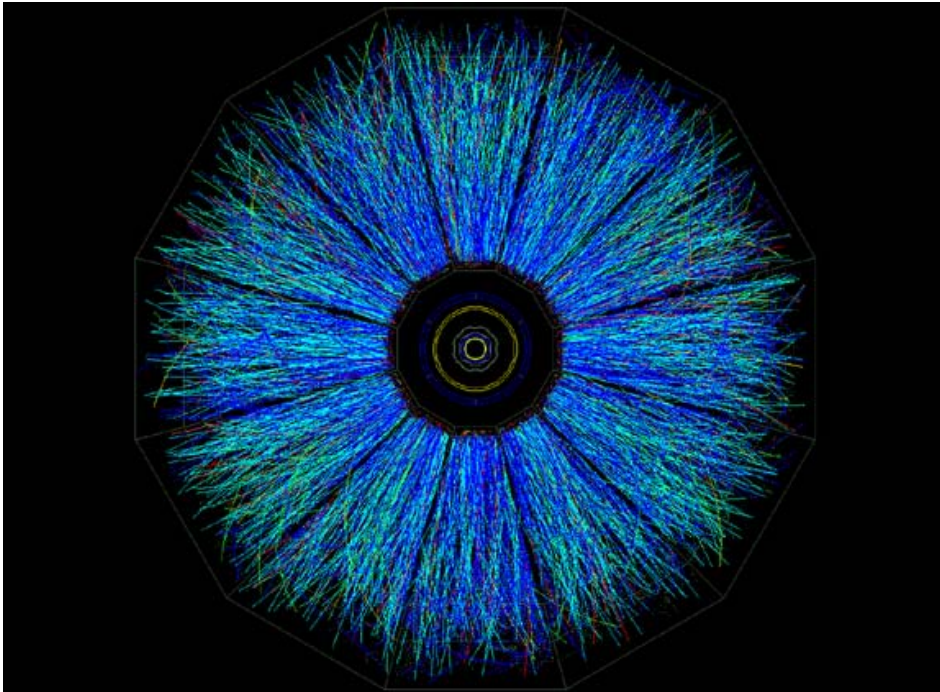


Fig. 3. Beam's eye view of a central event in the STAR Time Projection Chamber. This event was drawn by the STAR level-3 online display.

The fast detectors that provide input to the trigger system are a central trigger barrel (CTB) at $|\eta| < 1$ and zero-degree calorimeters (ZDC) located in the forward direction at $\theta < 2$ mrad. (In the future, additional detectors will be used as input to the trigger system.) The CTB surrounds the outer cylinder of the TPC, and

triggers on the flux of charged-particles in the midrapidity region. The ZDCs are used for determining the energy in neutral particles remaining in the forward directions. Each experiment at RHIC has a complement of ZDC's for triggering and cross-calibrating the centrality triggering between experiments [14]. Displayed in Figure 4 is the correlation between the summed ZDC pulse height and that of the CTB for events with a primary collision vertex successfully reconstructed from tracks in the TPC. The largest number of events occurs for large ZDC values and small CTB values (gray region of the plot). From simulations these correspond to collisions at large impact parameters, which occur most frequently and which characteristically leave a large amount of energy in the forward direction (into the ZDC) and a small amount of energy and particles sideward (into the CTB). Collisions at progressively smaller impact parameters occur less frequently and result in less energy in the forward direction (smaller pulse heights in ZDC) and more energy in the sideward direction (larger pulse heights in CTB). Thus, the correlation between the ZDC and CTB is a monotonic function that is used in the experiment to provide a trigger for centrality of the collision. The ZDC is double-valued since collisions at either small or large impact parameter can result in a small amount of energy in the forward ZDC direction.

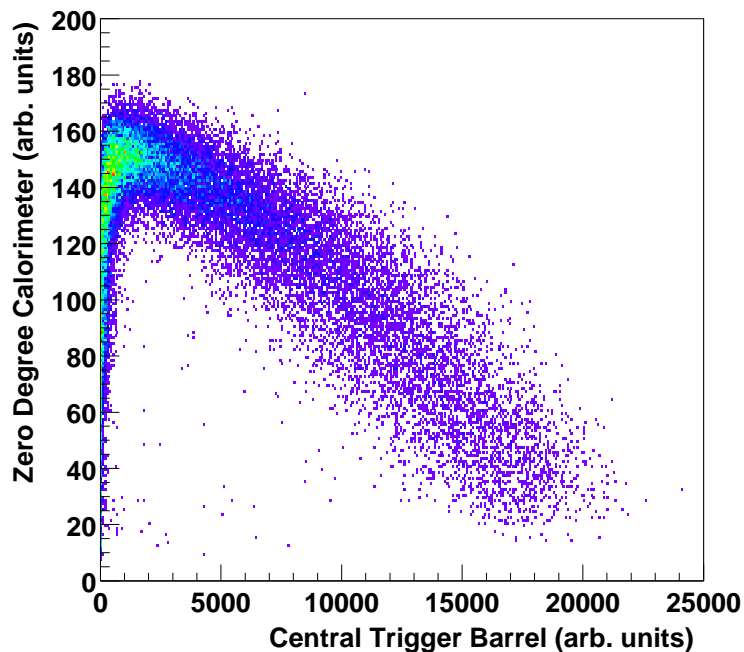


Fig. 4. Correlation between the summed pulse heights from the Zero Degree Calorimeters and the Central Trigger Barrel for events with a primary collision vertex successfully reconstructed from tracks in the Time Projection Chamber.

A minimum bias trigger was obtained by selecting events with a pulse height larger than that of one neutron in each of the forward ZDC's, which corresponds to 95 percent of the geometrical cross section. Triggers corresponding to smaller impact

parameter were implemented by selecting events with less energy in the forward ZDCs, but with sufficient CTB signal to eliminate the second branch at low CTB values shown in Figure 4.

4 Physics Overview

The STAR physics program at RHIC can be divided into three main categories: a study of high density QCD, measurement of the spin structure function of the proton, and a study of photon and pomeron interactions from electromagnetic fields of the passing ions at RHIC. RHIC and STAR were built initially to study high density QCD and to search for the QGP using ultra-relativistic heavy ion collisions. STAR will also study proton-proton interactions and proton-nucleus interactions in order to understand the initial parton distribution functions of the incident nuclei and for reference data for the heavy ion studies. By studying interactions of polarized protons at RHIC, STAR will determine the contributions from the preferential orientation of gluon spins to the overall spin of the proton, and we will map the flavor-dependence of antiquark polarizations in a polarized proton. Through the use of ultra-peripheral heavy ion interactions STAR will study photon and pomeron interactions resulting from the intense electromagnetic fields of the colliding ions and colorless strong interactions, respectively.

Inclusive p_t and η distributions of charged particles will be measured in STAR to investigate the degree of thermalization, contribution of collective flow, possible effects of disoriented chiral condensates, at low p_t , and nuclear effects and parton energy loss at high p_t . The p_t spectra of baryons and anti-baryons at mid-rapidity help determine the nuclear stopping power, baryon number transport, and establishes the baryo-chemical potential of the particle-emitting source at mid-rapidity. Global thermodynamic variables such as entropy, baryon and strangeness chemical potentials, temperature, energy density, and pressure can be associated with the multiparticle final state observables of pion multiplicity, net baryon distributions and strange particle abundance, mean transverse momentum, transverse energy and particle flow, respectively.

As a consequence of the large particle multiplicities in central collisions and the large acceptance of STAR, STAR will investigate nonstatistical (dynamical) fluctuations, deviations from global thermodynamic variables, and other significant departures from conventional hadronic physics. Color fluctuations in the early partonic stages of collision may result in significant dynamical variation in the produced particle spectra. Chiral symmetry restoration and nonequilibrium evolution of the collision system may produce chirally-disoriented domains in which the neutral-to-charged ratio of low- p_t pions deviates significantly from its nominal value.

Correlations between identical and non-identical pairs of particles will provide information on the freezeout geometry, the expansion dynamics and possibly the existence of a QGP. The dependence of the pion-emitting and kaon-emitting source parameters on the transverse momentum components of the particle pairs, and as a function of the various types of particle pairs will be measured with high statistics.

The hard scattering component becomes prominent at RHIC energies and is calculable in perturbative quantum chromodynamics (pQCD). This allows, for the first time in relativistic heavy ion collisions, the use of high transverse momentum processes (such as hard scattering of partons) in the form of high p_t jets, mini-jets and single particles to probe the properties of the medium through which they propagate.

In addition to the heavy ion program, STAR will utilize polarized proton-proton collisions to accumulate detailed information on the contribution of gluons to the spin of the proton. Recent results from polarized deep-inelastic scattering experiments indicate that the intrinsic spins of all the quarks and antiquarks combined can only account for a fraction (≈ 30 percent) of the overall spin of the nucleon. The STAR experiment is uniquely suited to measure the contribution due to gluons via the detection of photon-jet coincidence events at $p_t \geq 10$ GeV/c. If the quark and gluon spins together do not account for the nucleon spin, the only remaining source would be the relative orbital motion of the quarks and gluons. Thus, measurements of the spin substructure of the proton may lead beyond our current, still rudimentary understanding of the quark motion inside a nucleon. In addition to probing gluon polarization, STAR will study W^{pm} production in $\sqrt{s} = 500$ GeV polarized proton collisions to determine the flavor-dependence of antiquark polarization which is expected to be sensitive to the mechanism for dynamical chiral symmetry breaking in the proton.

STAR will also study ultra-peripheral collisions, where the nuclei physically miss each other, but interact via longer ranged forces that couple coherently to the nucleons[15]. The best known example of this is two-photon collisions, studied at e^+e^- colliders. Photon-Pomeron interactions will also be studied.

At the time of submission of this article the first physics results from RHIC have started to emerge. Initial results from STAR have been reported in [16–22], with the anticipation of many new physics results to come. In the remainder of this volume, the STAR detector subsystems will be described in detail in individual articles.

Acknowledgements

We wish to thank the RHIC Operations Group and the RHIC Computing Facility at Brookhaven National Laboratory, and the National Energy Research Scientific

Computing Center at Lawrence Berkeley National Laboratory for their support. This work was supported by the Division of Nuclear Physics and the Division of High Energy Physics of the Office of Science of the U.S. Department of Energy, the United States National Science Foundation, the Bundesministerium fuer Bildung und Forschung of Germany, the Institut National de la Physique Nucleaire et de la Physique des Particules of France, the United Kingdom Engineering and Physical Sciences Research Council, Fundacao de Amparo a Pesquisa do Estado de Sao Paulo, Brazil, the Russian Ministry of Science and Technology and the Ministry of Education of China and the National Science Foundation of China.

References

- [1] ‘Conceptual Design Report for the Solenoidal Tracker At RHIC’, The STAR Collaboration, PUB-5347 (1992); J.W. Harris et al, Nucl. Phys. A 566, 277c (1994).
- [2] R.L. Brown et al., Proc. 1997 IEEE Particle Accelerator Conf., 3230 (1998) and F. Bergsma et al., ‘The STAR Detector Magnet Subsystem’, (this volume).
- [3] D. Lynn et al., Nucl. Instrum. Meth. A447, 264 (2000) and R. Bellwied et al., ‘The STAR Silicon Vertex Tracker’, (this volume).
- [4] L. Arnold et al., ‘The STAR Silicon Strip Detector’, (this volume).
- [5] H. Wieman et al., IEEE Trans. Nucl. Sci. 44, 671 (1997) and M. Anderson et al., ‘The STAR Time Projection Chamber’, (this volume).
- [6] S. Klein et al., IEEE Trans. Nucl. Sci. 43, 1768 (1996) and M. Anderson et al., ‘A Readout System for the STAR Time Projection Chamber’, (this volume).
- [7] A. Schuttauf et al., Nuc. Phys. A661, 677c (1999) and K.H. Ackerman et al., ‘The Forward Time Projection Chamber in STAR’, (this volume).
- [8] ‘A Ring Imaging Cherenkov Detector for STAR’, STARnote 349, STAR/ALICE RICH Collaboration (1998); ALICE Collaboration, Technical Design and Report, Detector for High Momentum PID, CERN/LHCC 98-19.
- [9] M. Beddo et al., ‘The STAR Barrel Electromagnetic Calorimeter’, (this volume).
- [10] C.E. Allgower et al., ‘The STAR Endcap Electromagnetic Calorimeter’, (this volume).
- [11] A. Ljubicic et al., IEEE Trans. Nucl. Sci. 47, 99 (2000) and J.M. Landgraf et al., ‘An Overview of the STAR DAQ System’, (this volume).
- [12] F.S. Beiser et al., ‘The STAR Trigger’, (this volume).
- [13] J.S. Lange et al., IEEE Trans. Nucl. Sci. 48, 3 (2000) and C. Adler et al., ‘The STAR Level-3 Trigger System’, (this volume).

- [14] ‘The RHIC Zero Degree Calorimeter’, C. Adler, A. Denisov, E. Garcia, M. Murray, H. Strobele, and S. White, Nucl. Instrum. Meth. A470, 488 (2001).
- [15] S. R. Klein and J. Nystrand, Phys. Rev. C 60, 014903 (1999).
- [16] ‘Elliptic Flow in Au+Au Collisions at $\sqrt{s_{nn}} = 130$ GeV’, K.H. Ackermann et al. (STAR Collaboration), Phys. Rev. Lett. 86, 402-407 (2001).
- [17] ‘Midrapidity Antiproton-to-Proton Ratio from Au+Au at $\sqrt{s_{nn}} = 130$ GeV’, C. Adler et al. (STAR Collaboration), Phys. Rev. Lett. 86, 4778-4782 (2001).
- [18] ‘Pion Interferometry of $\sqrt{s_{nn}} = 130$ GeV Au+Au Collisions at RHIC’, C. Adler et al. (STAR Collaboration), Phys. Rev. Lett. 87, 082301 (2001).
- [19] ‘Multiplicity Distribution and Spectra of Negatively Charged Hadrons in Au+Au Collisions at $\sqrt{s_{nn}} = 130$ GeV’, C. Adler et al. (STAR Collaboration), Phys. Rev. Lett. 87, 112303 (2001).
- [20] ‘Identified Particle Elliptic Flow in Au+Au Collisions at $\sqrt{s_{nn}} = 130$ GeV’, C. Adler et al. (STAR Collaboration), Phys. Rev. Lett. 87, 182301 (2001).
- [21] ‘Antideuteron and Antihelium Production in Au+Au Collisions at $\sqrt{s_{nn}} = 130$ GeV’, C. Adler et al. (STAR Collaboration), Phys. Rev. Lett. 87, 262301-1 (2001).
- [22] ‘Measurement of Inclusive Antiprotons from Au+Au Collisions at $\sqrt{s_{nn}} = 130$ GeV’, C. Adler et al. (STAR Collaboration), Phys. Rev. Lett. 87, 262302-1 (2001).